Measurement of Path Loss Characterization and Prediction Modeling for Swarm UAVs Air-to-Air Wireless Communication Systems

Sarun Duangsuwan
Electrical Engineering, Department of Engineering, King Mongkut's Institute of Technology Ladkrabang, Prince of Chumphon Campus, 17/1 Chumcoo District, Pathio, Chumphon, Thailand
Email: sarun.du@kmitl.ac.th

Abstract —A challenge swarm unmanned aerial vehicles (swarm UAVs)-based wireless communication systems have been focused on channel modeling in various environments. In this paper, we present the characterized path loss air-to-air (A2A) channel modeling-based measurement and prediction model. The channel model was considered using A2A Two-Ray (A2AT-R) extended path loss modeling. The prediction model was considered using an artificial neural network (ANN) algorithm to train the measured dataset. To evaluate the measurement result, path loss models between the A2AT-R model and the prediction model are shown. We show that the prediction model using ANN is optimal to train the measured data for the A2A channel model. To discuss the result, the parametric prediction errors such as mean absolute error (MAE), root mean square error (RMSE), and R-square (R^2), are performed.

Index Terms—Path loss characterization, prediction model, air-to-air wireless communication system, ANN algorithm, swarm UAVs.

I. Introduction

Most recently, UAVs or drones have become inherently equipped with important communications [1], computer vision [2], and machine learning techniques [3] that turned them into truly autonomous and multipurpose devices. In general, all types of UAVs can be equipped with wireless interfaces. Such interfaces can operate at either unlicensed, Wi-Fi, or cellular frequencies. A new application domain for UAVs wireless communications and networks are: (a) UAVs as aerial base station [4] or access points that can be deployed to handle wireless networking and communications capabilities to a various geographical area [5], (b) UAVs can provide the existing infrastructure (5G or Wi-Fi) to communicate with ground devices [6], (c) UAVs can be applied as aerial relays communications to extend the coverage and connectivity.

In the use case of UAVs as an aerial base station (ABS), the air-to-ground wireless channel needs a new propagation environment whose parameters such as path loss, angular spread, and delay spread are significantly analyzed [7]-[10]. The propagation modeling and measurements are important research challenges for UAVs-ABS [11]-[14]. Meanwhile, A2A wireless channel is a new application in this group for communication between multiple UAVs. Therefore, the path loss characteristic of A2A channel modeling is taken into account for UAV-to-UAV wireless communication systems.

In this paper, the major contributions and novelties are summarized by

(1) The path loss characterization and prediction model are studied and measured for swarm UAVs A2A-based wireless communication systems.

(2) The prediction model by using the ANN algorithm is proposed to compare with the A2AT-R model and the Log-distance model. Moreover, the prediction errors such as MAE, RMSE, and R^2, are performed.

The remainder of this paper is organized as follows. Section II presents the related works. Section III presents the methodology. Section IV describes the measurement setup. Section V presents the model validation and result. At last, conclusions are drawn in Section IV.

II. Related Works

A ray-tracing simulation for UAV A2A channel modeling at 2.4 GHz was presented in [15] for urban environments. The authors presented the simulation with a fixed transmitter and moving receiver with 100 m radius and 3 km distance. They derive the Log-distance path loss model and characterize the small-scale fading by Rician fading. To characterize the delay spread, they show the excess delay of the multipath component within 6 dB, 12 dB, and 18 dB below the line-of-sight (LOS) component, all the excess delayed paths arrive within 570 ns for 3 km distance and 500 m height. However, the authors have discussed that the A2A channel modeling of Wi-Fi 2.4 GHz was higher power loss over the sea than the land.

Then, the fixed-wing small UAVs at 5 GHz A2A channel modeling was performed in [16] over the ground and the sea. The authors consider both LOS and multipath channels. They discuss that the delay spread above the sea was higher than the ground. In previous work, the authors have analyzed at 2.3 GHz frequency with an altitude lower than 1.5 km in [17]. The

Manuscript received December 22, 2020; revised May 21, 2021.
Corresponding author email: sarun.du@kmitl.ac.th.
doi:10.12720/jcm.16.6.228-235

measurement environments were conducted to examine ground conditions such as urban, suburban, trees, mountains, and over the seas. They reveal that ground reflection gives an impact on the path loss component for over the sea areas.

The cooperative relay-based UAVs-A2A channel was presented in [18]. Results show that Rayleigh channel fading was suitable for low altitude small UAVs, while Nakagami-*m* and Weibull channel fading was suitable for dense UAV areas and high altitudes open space. Besides, the performance of bit error rates (BER) was evaluated in [19], wherein scenario of a large Dropper shift with high-speed UAV frying was considered. Their results show that there is a 2 dB loss for Wi-Fi IEEE 802.11a signals at 5 GHz over the frequency selective fading channel.

The UAV-A2A channel modeling and prediction modeling have been proposed in research works [20]-[21]. In [20], two machine learning algorithms such as random forest (RF) and k-nearest neighbor (kNN) were presented for A2A path loss prediction models in an urban environment. The authors described the A2A channel modeling by using the ray-tracing method. To compare with the empirical model as SUI model and COST231-W-I model, it has been shown that machine learning provides a flexible modeling approach based on the training data for such a complex environment and RF has the best prediction performance. Although the RF and kNN can be predicted the path loss model in these scenarios, however, it depends on simulation parameters.

In [21], the authors proposed the measurement in the field of A2A channel modeling. The path loss characteristic based on the Log-distance model was presented. The measurement setup was similar to vehicle-to-vehicle (V2V) communication system-based UAV. Then, the path loss versus distance and fitting function of the path loss model at various altitudes were tested. It can be shown that the Log-distance path loss model is dependent on the distance between UAV-to-UAV setup, but there is no consideration to the ground reflection or any propagation multipath fading. However, the authors have discussed that the multipath fading was decreased where the UAV altitude was lower than 60 m. Therefore, the results of this work can serve as a reference for a new channel modeling of small UAVs-A2A channel.

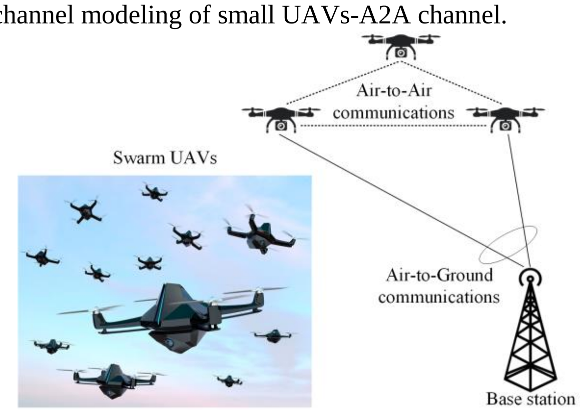

Fig. 1. The swarm UAVs channel models for wireless communication system.

As aforementioned above of research works, the most of A2A channel modeling is considered based on using Wi-Fi networking at 2.4 GHz or 5 GHz, path loss-based Log-distance modeling, different environments, and more accuracy of path loss model by using machine learning. However, the propagation challenge is not restricted to the swarm UAVs A2A wireless communication system as shown in Fig. 1.

III. Methodology

A. *Analytical A2AT-R Path Loss Model*

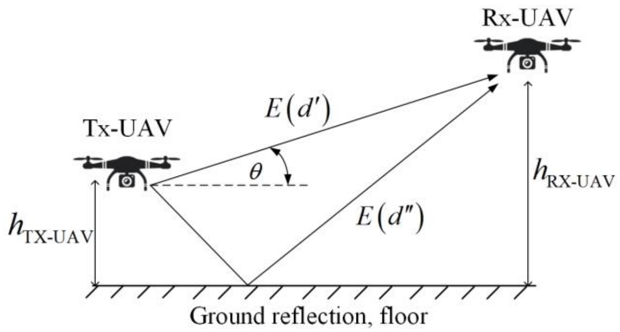

Fig. 2. The geometrics for the analytical A2AT-R model.

The propagation of A2A wireless channel between Tx-UAV and Rx-UAV can be analyzed using the analytical A2AT-R model. Fig. 2 shows the geometrics for the analytical A2AT-R model where the total received E-field at the Rx-UAV, is $E_U(d_c)$, then a result of the direct line-of-sight (LOS) component, $E(d')$, and the ground reflected component, $E_r(d'')$

$$E_U(d_c) = E(d') + E_r(d'') \tag{1}$$

To note that traveling two waves arrive at Rx-UAV: the direct wave that travels distance d'; and the reflected wave that travels distance d''. Thus, d_c is the distance between Tx-UAV and Rx-UAV. The E-field due to the LOS at the Rx-UAV can be expressed as

$$E(d') = \frac{E_0 d_0}{d'} \cos\left(2\pi f_c \left(t - \frac{d'}{c}\right)\right) \tag{2}$$

and the E-field for the ground reflected wave, which has a propagation distance of d'', can be expressed as

$$E_r(d'') = \Gamma_{Floor} \frac{E_0 d_0}{d''} \cos\left(2\pi f_c \left(t - \frac{d''}{c}\right)\right) \tag{3}$$

where f_c is the carrier frequency and c is the velocity of the light, and E_0 is the free space E-field at a reference distance d_0 from the GS, then $d > d_0$. Γ_{Floor} denotes the reflection coefficient from the floor.

The $E_U(d_c)$ can be rewritten as

$$E_U(d_c) = \frac{E_0 d_0}{d'}\cos\left(2\pi f_c\left(t - \frac{d'}{c}\right)\right) + (-1)\frac{E_0 d_0}{d''}\cos\left(2\pi f_c\left(t - \frac{d''}{c}\right)\right) \quad (4)$$

where $\Gamma_{Floor} = -1$ denotes the perfect ground reflection component from the floor.

In term of received signal strength indicator (RSSI), we obtain to the received signal of the empirical A2AT-R model, $r_{T-R}(t)$ can be written as

$$r_{T-R}(t) = \left(\frac{\lambda}{4\pi}\left|r_{d'}(t) + r_{d''}(t)\right| \cdot e^{j2\pi f_c t}\right) \quad (5)$$

where

$$r_{d'}(t) = \frac{\sqrt{G_{T,d'}G_{R,d'}}}{d_0} e^{-j2\pi\frac{d_0}{\lambda}} \cdot \left|E(d')\right|^2 \quad (6)$$

$$r_{d''}(t) = \frac{\sqrt{G_{T,d''}G_{R,d''}}}{d_0} e^{-j2\pi\frac{d_0}{\lambda}} \cdot \left|E_r(d'')\right|^2 \quad (7)$$

where $G_{T,d'}$ and $G_{R,d'}$ are the antenna field radiation patterns of the Tx-UAV and Rx-UAV antennas in LOS direction, respectively, $G_{T,d''}$ and $G_{R,d''}$ are the antenna field radiation patterns of the Tx-UAV and Rx-UAV antennas along the direction of the ground reflection path, respectively.

Denote by $h_{\text{Tx-UAV}}$ and $h_{\text{Rx-UAV}}$ the heights of the Tx-UAV and Rx-UAV, respectively. The propagation distance and the phase difference by difference of the LOS path and the ground reflection path, denoted by

$$\Delta d = \frac{2h_{\text{Tx-UAV}}h_{\text{Rx-UAV}}}{d_c} \quad (8)$$

$$\Delta\theta = \frac{4\pi h_{\text{Tx-UAV}}h_{\text{Rx-UAV}}}{\lambda d_c} \quad (9)$$

The received signal power can be approximately calculated as follows

$$P_{\text{Rx-UAV}}(d_c) \approx P_{\text{Tx-UAV}}\left(\frac{\lambda}{4\pi}\right)^2 \frac{G_T G_R}{d_c^2} \left(\frac{4\pi h_{\text{Tx-UAV}}h_{\text{Rx-UAV}}}{\lambda d_c}\right)^2 = P_{\text{Tx-UAV}} G_T G_R h_{\text{Tx-UAV}}^2 h_{\text{Rx-UAV}}^2 d_c^{-4} \quad (10)$$

where G_T denotes the approximate value for $G_{T,d'}$ and $G_{T,d''}$, G_R to denote the approximate value for $G_{R,d'}$ and $G_{R,d''}$, respectively.

The path loss-base analytical A2AT-R model, is given by

$$PL_{T-R} \approx \frac{1}{4G_T G_R}\left(\frac{4\pi d_c}{\lambda}\right)^2 \cdot \sin^{-2}\left(\frac{2\pi h_{\text{Tx-UAV}}h_{\text{Rx-UAV}}}{\lambda d_c}\right) \quad (11)$$

To compare the path loss characterization with Log-distance path loss model, it can be written as

$$PL_{Log}(\text{dB}) = 10\alpha\log_{10}(d_c) + \beta \quad (12)$$

where α is the slope that still bears the meaning of the path loss component and β denotes the intercept of measured data. The values of α and β are usually jointly determined by minimizing the means square error between the analytic model and empirical measurements.

B. Prediction Model

In this subsection, the prediction model is used to train the measured data by using ANN algorithms. We provide the ANN algorithm because it is a rapid computation to perform the training process in a supervised algorithm. The performance indicators [22] such as MAE, RMSE, and the coefficient of determination or R^2, are expressed as

$$\text{MAE} = \frac{1}{N}\sum_{i=1}^{N}\left|P_L^i - \hat{P}_L^i\right| \quad (13)$$

$$\text{RMSE} = \sqrt{\frac{1}{N}\sum_{i=1}^{N}\left[P_L^i - \hat{P}_L^i\right]^2} \quad (14)$$

$$R^2 = 1 - \frac{\sum_{i=1}^{N}\left[P_L^i - \hat{P}_L^i\right]}{\sum_{i=1}^{N}\left[P_L^i - \bar{P}_L^i\right]} \quad (15)$$

where N is the number of samples test, P_L is the measured path loss data, and $\hat{P}_L$ is the training path loss data from prediction model. The $\bar{P}_L$ is the average mean of path loss from the prediction model.

The block diagram of data processing is shown in Fig. 3. The measured datasets are considered as RSSI and path loss to train the data for both the A2AT-R model and prediction model. In the prediction model, there are three sections including the training process, predicting, and validation model. A MATLAB program was used to calculate the MAE, RMSE, and R^2 respectively. Finally, the model validation of RSSI and path loss results are shown.

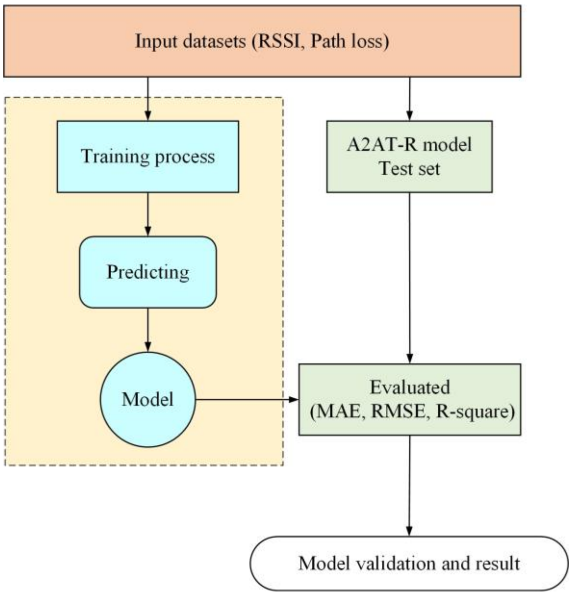

Fig. 3. Block diagram of the data processing between A2AT-R model and prediction model.

The proposed ANN algorithm is modeled as

Input: Dataset $x = [\mathbf{x}_1, \mathbf{x}_2, \ldots, \mathbf{x}_N]$ is both RSSI and path loss measured data.

Training Process:

For *j = 1 to k*

(1) Define the input layers as $k = 50$ and one hidden layer with 50 neurons.

(2) The output layer of ANN is expressed by $y = f\left(\sum_{j=1}^{k} \mathbf{w}_j \left(f\left(\sum_{i=1}^{N} \mathbf{w}_i \mathbf{x}_i\right)\right)\right)$.

Predicting:

(3) The y is predicted by using sigmoid and linear activation function, assuming that the least square is $\hat{P}_L = \frac{1}{N}\sum_{i=1}^{N}\left(P_L^i - y\right)^2$.

Model:

(4) Calculate MAE, RMSE, and R^2, respectively.

(5) End program.

IV. Measurement Setup

The measurement setup was considered in the different ground reflection conditions such as Grass floor, Soil floor, and Rubber floor, respectively, as shown in Fig. 4. We set the Tx-UAV at 1 m altitude fixed and moved the Rx-UAV hover up from 1 m to 10 m altitudes. The flight time of both Tx-UAV and Rx-UAV was fifteen minutes, the prototype of Tx-UAV and Rx-UAV is shown in Fig. 5, where the Tx-wireless and Rx-wireless modules were equipped on the Tx-UAV and Rx-UAV based on Wi-Fi 2.4 GHz frequency.

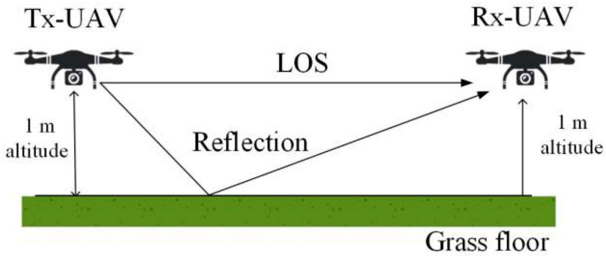

(a) Ground reflection from grass floor.

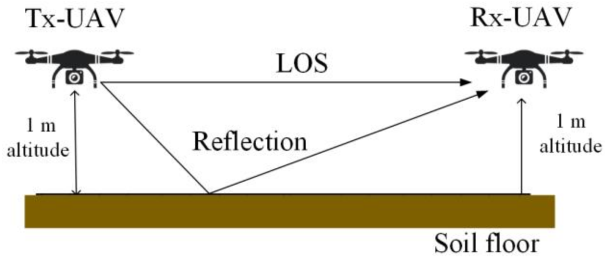

(b) Ground reflection from soil floor.

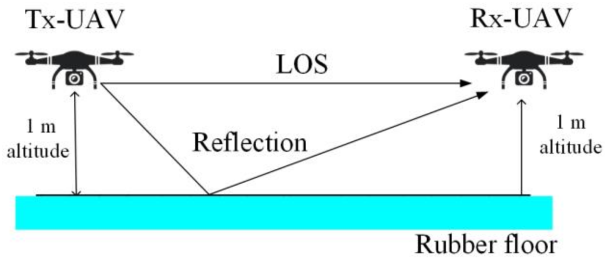

(c) Ground reflection from rubber floor.

Fig. 4. Different of ground reflections in the measurement setup.

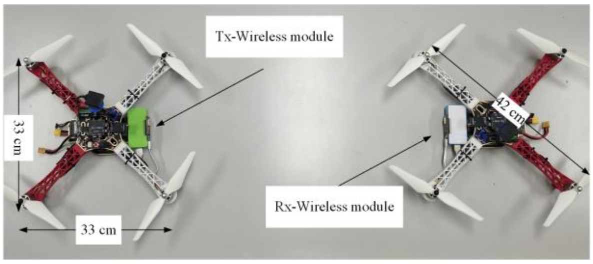

Fig. 5. Prototype of Tx-UAV and Rx-UAV.

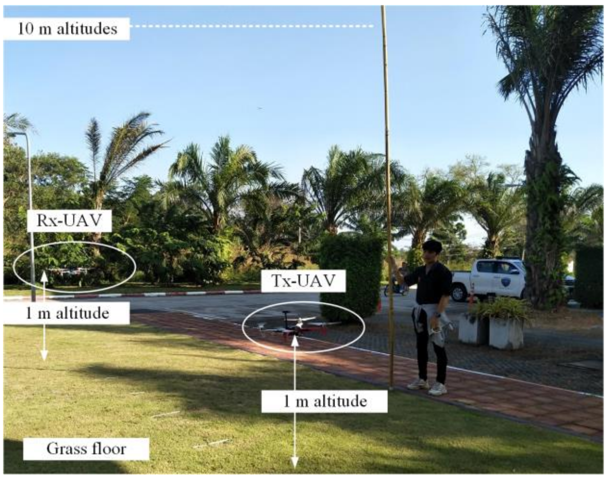

(a) Grass floor.

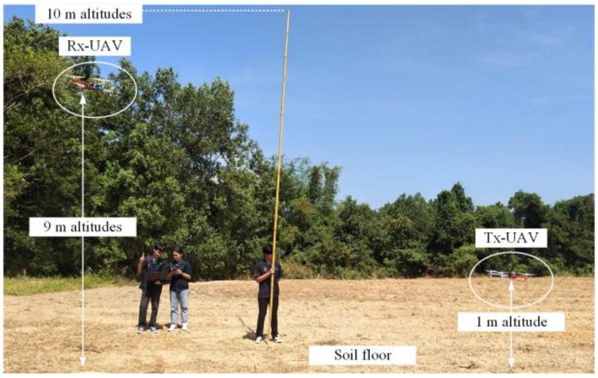

(b) Soil floor.

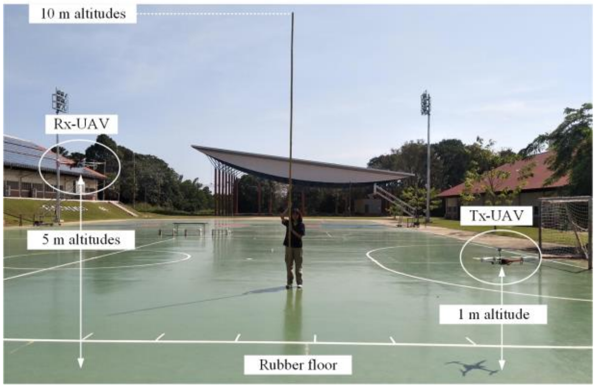

(c) Rubber floor.

Fig. 6. Measurement between Tx-UAV and Rx-UAV testbed based different ground reflection conditions.

TABLE I: MEASUREMENT SETUP PARAMETERS

Description	Values
Carrier frequency	2.400 – 2.480 GHz
Bandwidth	20 MHz
Tx-UAV Transmit power	20 dBm
Tx-UAV altitude	1 m
Rx-UAV alttitude	1-10 m
Distance between Tx-UAV and Rx-UAV	5 m
UAV flight time	15 min
Antenna gain	3.1 dBi

Fig. 6 shows the measurement setup between Tx-UAV and Rx-UAV testbed based on different ground reflection conditions, where the condition in Grass floor as shown in Fig. 6 (a), Soil floor in Fig. 6 (b), and Rubber floor in Fig. 6(c), respectively. The measurement setup parameters are shown in Table I. To evaluate the RSSI and path loss results, we set the transmit power of the Tx-UAV wireless module at 20 dBm and fixed the altitude at 1 m. Then, the Rx-UAV was hovered up from 1 m until 10 m altitudes. We obtain the separation distance between Tx-UAV and Rx-UAV was set at 5 m, and it depends on the propagation distance Δd when Rx-UAV hovering up.

V. MODEL VALIDATION AND RESULT

In this section, the model of RSSI and path loss are characterized. To examine the validity of the proposed models, the results of RSSI and path loss are validated with the empirical A2AT-R model and prediction model.

Fig. 7 shows the RSSI versus Rx-UAV altitudes in different ground reflection conditions. The Grass floor condition is shown in Fig. 7(a) where the empirical A2AT-R model is expressed at -21.23 dBm to -44.54 dBm versus Rx-UAV altitudes. While the measured data of RSSI results are shown at -24.12 dBm to -44.32 dBm. We show the prediction errors in Table II where MAE is 5.120 dB, 6.123 dB RMSE, and 0.653 R^2. It can be realized that A2AT-R model and measured data are similar to 65 %. Additionally, the predicted by ANN algorithm is the lowest of prediction errors where MAE is 1.124 dB, 2.132 dB RMSE, and 0.975 R^2, respectively. It can show that ANN algorithm is optimal to predict the accuracy of RSSI to 97 % compared with the A2AT-R model. In Fig. 7(b), we plot the RSSI from the Soil floor. The RSSI versus Rx-UAV altitudes are -24.76 dBm to -44.98 dBm. We observe that a comparison between the empirical A2AT-R model and the measured data is different than the Grass floor in Fig. 7(a) because it depends on the propagation environment. Similarly, the RSSI measured data of the Rubber floor is shown in Fig. 7(c) where RSSI is -25.21 dBm to -48.32 dBm. The prediction errors in both soil and rubber floor are shown in Table II. It can be seen that the effect of ground reflection from the rubber floor occurs at 1 m to 2 m of Rx-UAV altitudes. On the other hand, it has no ground reflection situation from the grass and soil floor. Thus, the fluctuated RSSI from ground reflection is shown in Fig. 7(c) at 1 m to 2 m Rx-UAV altitudes.

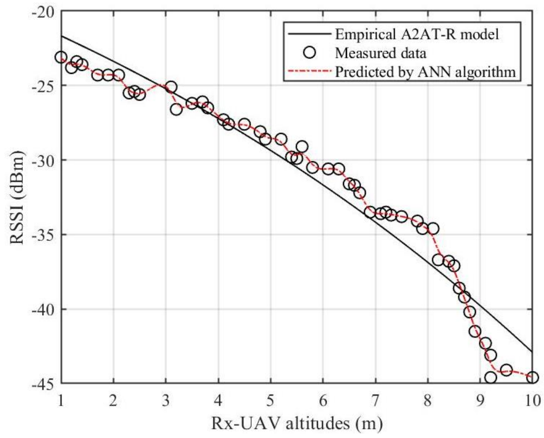

(a) Grass floor.

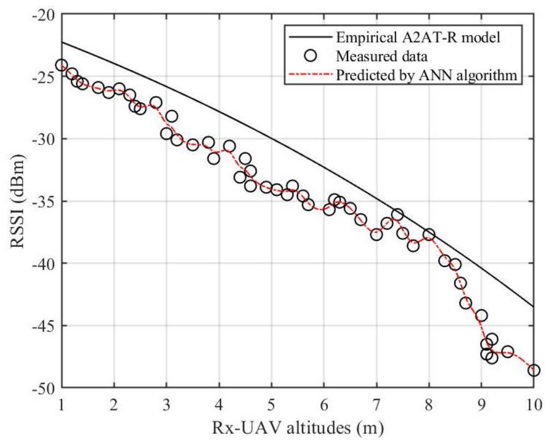

(b) Soil floor.

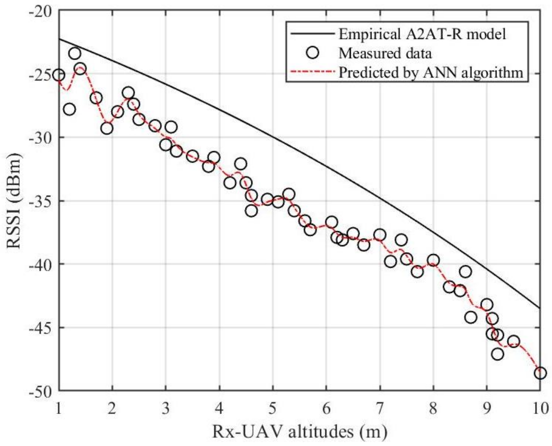

(c) Rubber floor.

Fig. 7. RSSI versus Rx-UAV altitudes in different ground reflection conditions.

Fig. 8 shows the path loss versus Rx-UAV altitudes in different ground reflection conditions. Path loss curves show such as the empirical A2AT-R model, measured data, Log-distance model [14], and predicted by ANN algorithm, respectively. The path loss A2AT-R model is analyzed from Equation (11) where the curve ranges from 10.43 dB to 21.57 dB versus Rx-UAV altitudes.

TABLE II: PREDICTION ERRORS OF RSSI

Models	Floors	MAE	RMSE	R^2
A2AT-R	Grass	5.120	6.123	0.653
	Soil	6.321	7.221	0.441
	Rubber	6.824	7.545	0.412
Predicted	Grass	1.124	2.132	0.975
	Soil	1.112	2.122	0.976
	Rubber	1.553	2.846	0.957

TABLE III: PREDICTION ERRORS OF PATH LOSS

Models	Floors	MAE	RMSE	R^2
A2AT-R	Grass	5.232	6.545	0.624
	Soil	4.664	5.573	0.625
	Rubber	4.632	5.633	0.602
Log-distance	Grass	2.124	4.212	0.754
	Soil	2.214	4.355	0.767
	Rubber	2.312	4.426	0.748
Predicted	Grass	1.125	2.251	0.975
	Soil	1.024	2.023	0.975
	Rubber	1.322	2.722	0.953

In Fig. 8(a), we plot the path loss values of the Grass floor where the measured data is varied from 12.54 dB to 30.21 dB and the model of Log-distance is 11.21 dB to 26.32 dB. We note that the path loss component α of Log-distance model was 2 for free-space environment. After that, we show the path loss curves of the Soil floor in Fig. 8(b). The result of Log-distance path loss model is 12.13 dB to 25.67 dB versus Rx-UAV altitudes. On the other hand, the predicted by ANN algorithm is 12.35 dB to 26.32 dB path loss curve. To compare the accuracy of prediction errors, it can be seen that the prediction error parameters of the predicted by ANN algorithm is lower than Log-distance model where the performance of R^2 is approximately performed to 0.975 or 97 % as shown in Table III. In Fig. 8(c), we observe that the effect of ground reflection fluctuates at 1 m to 3 m Rx-UAV altitudes from the prediction model. Therefore, we distinguish that the ground reflection of Rubber floor has been affected more than the Grass and Soil floor at 1 m to 3 m Rx-UAV altitude from our measurement data. Additionally, the prediction errors are shown in Table III.

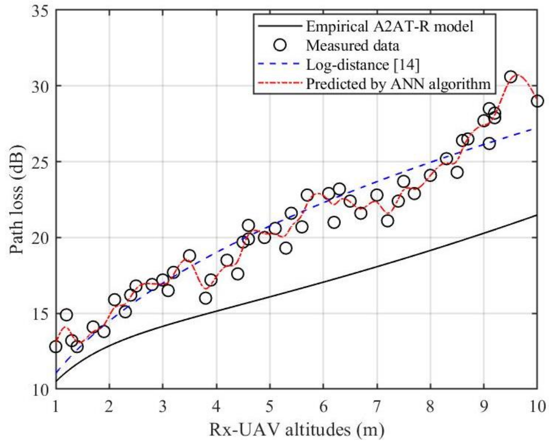

(a) Grass floor.

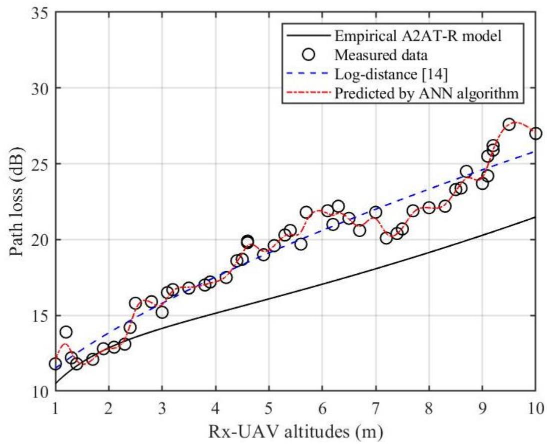

(b) Soil floor.

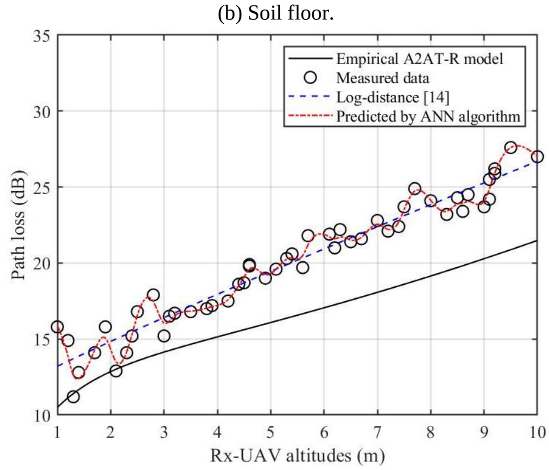

(c) Rubber floor.

Fig. 8. Path loss versus Rx-UAV altitudes in different ground reflection conditions.

To discuss the prediction modeling, we clarify that the predicted by ANN algorithm can optimal more accuracy of path loss measurement where the lowest of MAE at 1.322 dB, 2.722 dB RMSE, and 0.953 R^2 or 95 % of efficiency. Although the A2AT-R model and the prediction model are different both RSSI and path loss values. However, the A2AT-R model and prediction modeling can be accomplished for swarm UAVs A2A channel modeling based on measurement of path loss characterization.

VI. Conclusion

In this paper, we have presented the measurement of path loss characterization and prediction modeling for swarm UAVs A2A wireless communication systems. The empirical A2AT-R model is analyzed to compare with Log-distance model and predicted by the ANN algorithm in different ground reflection conditions such as Grass floor, Soil floor, and Rubber floor, respectively. Based on our measuring results, it has been shown that RSSI and path loss modeling relates the propagation distance over varying Rx-UAV altitudes and Rubber floor has more reflection coefficient than other floors. The results of our work can serve as a reference for the swarm UAV A2A channel modeling-based empirical measurement model.

To study future work, the A2A channel modeling for UAVs-enabled wireless communication by using the LoRa communication module at 868 MHz frequency will be investigated by the path loss characterization.

Conflict of Interest

The author declares that there are no conflicts of interest concerning the publication of this paper.

Acknowledgement

This work was financially supported by a KMITL research fund, and included in the Academic Melting Pot scholarship project.

References

[1] Z. Yuan, J. Jin, L. Sun, K. W. Chin, and G. M. Muntean, "Ultra-reliable IoT communications with UAVs: A swarm use case," *IEEE Communications Magazine*, vol. 56, vol. 12, pp. 90-96, 2018.

[2] F. Schilling, J. Lecoeur, F. Schiano, and D. Floreano, "Learning vision-based flight in drone swarms by imitation," *IEEE Robotics and Automation Letters*, vol. 4, no. 4, pp. 4523-4530, 2019.

[3] L. Shan, R. Miura, T. Kagawa, F. Ono, H. B. Li, and F. Kojima, "Machine learning-based field data analysis and modeling for drone communications," *IEEE Access*, vol. 7, pp. 79127-79135, 2019.

[4] S. Duangsuwan, C. Teekapakvisit, and M. M. Maw, "Development of soil moisture monitoring by using IoT and UAV-SC for smart farming application," *Advances in Science, Technology and Engineering Systems Journal (ASTESJ)*, vol. 5, no. 4, pp. 381-387, 2020.

[5] Z. Xiao, P. Xia, and X. G. Xia, "Enabling UAV cellular with millimeter-wave communication: Potentials and approaches," *IEEE Communications Mag.*, vol. 54, pp. 66-73, May 2016.

[6] S. Duangsuwan, and M. M. Maw, "Comparison of path loss prediction models for UAV and IoT air-to-ground communication system in rural precision farming environment," *Journal of Communications*, vol. 16, no. 2, pp. 60-66, 2021.

[7] G. Athanasiadou and G. V. Tsoulos, "Path loss characteristics for UAV-to-ground wireless channels," in *Proc. 13th European Conference on Antennas and Propagation (EuCAP)*, Krakow, Poland, Apr. 2019, pp. 1-4.

[8] W. H. Jeong, H. R. Choi and K. S. Kim, "Empirical path-loss modeling and a RF detection scheme for various drones," *Wireless Communications and Mobile Computing*, vol. 2018, pp. 1-13, 2018.

[9] M. Bacco, A. Berton, A. Gotta and L. Caviglione, "IEEE 802.15.4 air-ground UAV communications in smart farming scenarios," *IEEE Communications Letters*, vol. 22, no. 9, pp. 1910-1913, 2018.

[10] J. Tharane, D. Zibar, and H. L. Christiansen, "Model-aided deep learning methods for path loss prediction in mobile communication systems at 2.6 GHz," *IEEE Access*, vol. 8, pp. 7925-7936, 2020.

[11] R. Amorim, H. Nguyen, P. Mogensen, I. Z. Kovács, J. Wigard, and T. B. Sørensen, "Radio channel modeling for UAV communication over cellular networks," *IEEE Wireless Communications Letters*, vol. 6, no. 4, pp. 514–517, 2017.

[12] Y. Shi, R. Enami, J. Wensowitch, and J. Camp, "Measurement-based characterization of LOS and NLOS drone-to-ground channels," in *Proc. IEEE Wireless Communications and Networking Conf.*, Spain, Apr. 2018, pp. 1-6.

[13] D. W. Matolak, and U. C. Fiebig, "UAV channel model: Review and future research," in *Proc. European Conf. on Antennas and Propagation*, Poland, Apr. 2019, pp. 1-5.

[14] W. Khawaja, I. Guvenc, D. W. Matolok, U. C. Fiedig, and N. Schneckenburger, "A survey of air-to-ground propagation channel modeling for unmanned aerial vehicles," *IEEE Communications Surveys & Tutorials*, vol. 21, no. 3, pp. 2361-2391, Third Quarter 2019.

[15] L. Zhou, Z. Yang, G. Zhao, S. Zhou, and C. X. Wang, "Propagation characteristics of Air-to-Air channels in urban environments," in *Proc. IEEE Global Communications Conf.*, United Arab Emirates, 2018, pp. 1-6.

[16] F. Ono, T. Kagawa, H. Tsuji, R. Miura, and F. Kojima, "Measurements on C-band air-to-air channel for coexistence among multiple unmanned aircraft systems," in *Proc. International Conf. on Unmanned Aircraft Systems*, USA, Jun. 2017, pp. 1160-1164.

[17] K. Takizawa, F. Ono, M. Suzuki, H. Tsuji, and R. Miura, "Measurement on S-band radio propagation characteristics for unmanned aircraft systems," in *Proc. European Conf. on Antennas and Propagation (EuCAP)*, Netherlands, Apr. 2014, pp. 3068-3072.

[18] Z. Ma, B. Ai, R. He, G. Wang, Y. Niu, and Z. Zhong, "A wideband non-stationary air-to-air channel model for UAV communications," *IEEE Transactions on Vehicular Tech.*, vol. 69, no. 2, pp. 1214-1226, Feb. 2020.

[19] X. Chen, X. Hu, Q. Zhu, W. Zhong, and B. Chen, "Channel modeling and performance analysis for UAV

relay systems," *China Communications.*, vol. 15, no. 12, pp. 89-97, Dec. 2018.

[20] Y. Zhang, J. Wen, G. Yang, Z. He, and X. Luo, "Air-to-air path loss prediction based on machine learning methods in urban environments," *Wireless Communications and Mobile Computing*, vol. 2018, pp. 1-10, 2018.

[21] T. Liu, Z. Zhang, H. Jiang, Y. Qian, K. Liu, J. Dang, and L. Wu, "Measurement-based characterization and modeling for low-altitude UAV air-to-air channels," *IEEE Access*, vol. 7, pp. 98832-98840, Jul. 2019.

[22] S. K. Goudos, G. Athanasiadou, G. V. Tsoulos, and V. Rekkas, "Modeling ray tracing propagation data using different machine learning algorithms," in *Proc. 14th European Conference on Antennas and Propagation (EuCAP)*, pp. 1 – 4, Copenhagen, Denmark, Mar. 2020.

Sarun Duangsuwan received the B.Eng. and M. Eng. degrees in Information Engineering from the King Mongkut's Institute of Technology Ladkrabang (KMITL), Thailand, in 2008, 2010, respectively, and the D.Eng. degree in Electrical Engineering in 2015 from KMITL, Thailand. Since 2016, he has worked with Electrical Engineering, KMITL, Prince of Chumphon Campus, Thailand. He is a head of Innovative Wireless and IoT Laboratory (IWIoT), Electrical Engineering, Department of Engineering, KMITL, Prince of Chumphon Campus. His research interests include IoT networks, UAV communication systems, air-to-ground channel modeling, air-to-air channel modeling, applied machine learning methods, wireless communications, MIMO, 5G communication systems, and signal processing.